

# NBTXR3 Radiotherapy-Activated Functionalized Hafnium Oxide Nanoparticles Show Efficient Antitumor Effects Across a Large Panel of Human Cancer Models

This article was published in the following Dove Press journal:  
*International Journal of Nanomedicine*

Ping Zhang<sup>1</sup>  
Julie Marill<sup>1</sup>  
Audrey Darmon<sup>1</sup>  
Naeemunnisa Mohamed  
Anesary<sup>1</sup>  
Bo Lu<sup>2</sup>  
Sébastien Paris<sup>1</sup> 

<sup>1</sup>Nanobiotix, Paris, France; <sup>2</sup>Department of Radiation Oncology, Thomas Jefferson University, Philadelphia, PA, 19107, USA

**Purpose:** The side effects of radiotherapy induced on healthy tissue limit its use. To overcome this issue and fully exploit the potential of radiotherapy to treat cancers, the first-in-class radioenhancer NBTXR3 (functionalized hafnium oxide nanoparticles) has been designed to amplify the effects of radiotherapy.

**Patients and Methods:** Thanks to its physical mode of action, NBTXR3 has the potential to be used to treat any type of solid tumor. Here we demonstrate that NBTXR3 can be used to treat a wide variety of solid cancers. For this, we evaluated different parameters on a large panel of human cancer models, such as nanoparticle endocytosis, in vitro cell death induction, dispersion, and retention of NBTXR3 in the tumor tissue and tumor growth control.

**Results:** Whatever the model considered, we show that NBTXR3 was internalized by cancer cells and persisted within the tumors throughout radiotherapy treatment. NBTXR3 activated by radiotherapy was also more effective in destroying cancer cells and in controlling tumor growth than radiotherapy alone. Beyond the effects of NBTXR3 as single agent, we show that the antitumor efficacy of cisplatin-based chemoradiotherapy treatment was improved when combined with NBTXR3.

**Conclusion:** These data support that NBTXR3 could be universally used to treat solid cancers when radiotherapy is indicated, opening promising new therapeutic perspectives of treatment for the benefit of many patients.

**Keywords:** radiotherapy, radioenhancer, nanoparticle, NBTXR3, cancer

## Introduction

Currently, approximately 50% of cancer patients will receive radiotherapy (RT) as part of their treatment.<sup>1</sup> Despite progress in development of radiotherapeutic oncology, computer technology and medical imaging technology, the undesirable effects of RT on healthy peripheral tissues still limits the dose usable in patients. The recent development of the first-in-class radioenhancer NBTXR3 (functionalized hafnium oxide nanoparticles) opened new avenues to address this major therapeutic issue. NBTXR3 is administered by a single intratumoral injection before RT. Before RT, NBTXR3 is inert (“off” status) but during RT treatment, the high electron density of NBTXR3 allows a high probability of interaction with incoming ionizing radiation, increasing energy dose deposit within cells (“on” status). Thanks to its physical mode of action, RT-activated NBTXR3 (NBTXR3+RT) is expected to be effective in all types of solid

Correspondence: Sébastien Paris  
Nanobiotix, 60 rue de Wattignies, Paris,  
75012, France  
Tel +33 | 75 44 72 33  
Fax +33 | 40 26 04 44  
Email [sebastien.paris@nanobiotix.com](mailto:sebastien.paris@nanobiotix.com)

tumors. NBTXR3 can therefore lead to either better efficacy with the same radiation dose<sup>2-4</sup> or similar efficacy than RT with a lower radiation dose. Antitumor efficacy of NBTXR3 +RT was demonstrated in a subset of tumors in preclinical settings,<sup>2,4</sup> and more recently demonstrated clinically meaningful benefit for patients with locally advanced Soft Tissue Sarcoma compared to RT alone, in the randomized controlled Phase II/III Act.in.Sarc study (NCT02379845).<sup>5</sup> Other nanoparticles using atoms with high electron density, such as gold nanoparticles, eg, are currently under development in the field of radiotherapy.<sup>6-9</sup>

In this article, we sought to demonstrate that NBTXR3 could be used to effectively treat any type of solid tumor, using a large panel of human tumors originating from different organs/tissues. We analyzed the capacity of these nanoparticles to be internalized by cancer cells and their retention within the tumors after intratumoral injection. We also studied the ability of NBTXR3+RT to improve cancer cell destruction and tumor growth control, compared to RT alone. In all the cancer cell lines tested here, NBTXR3+RT showed greater efficacy than RT alone. We also demonstrated that NBTXR3 can improve the efficiency of chemoradiation treatment with cisplatin (CDDP).

## Materials and Methods

### Cell Culture and Reagents

The human cancer cell lines Detroit 562 (#CCL-138, pharyngeal carcinoma), FaDu (#HTB-43, squamous cell pharyngeal carcinoma), HT1080 (#CCL-121, fibrosarcoma), MIA PaCa-2 (#CRL-1420, pancreas carcinoma), NCI-H460 (#HTB-177, large cell lung carcinoma) and T98G (#CRL-1690, glioblastoma) were purchased from ATCC. The human cancer cell lines CAL-33 (#ACC 447, tongue squamous cell carcinoma), DU-145 (#ACC 261, prostate carcinoma), HEP-3B (#ACC 93, hepatocellular carcinoma), LNCaP (#ACC 256, prostate carcinoma) and PC-3 (#ACC 465, prostate adenocarcinoma) were purchased from DSMZ. The human cancer cell lines MDA-MB-231-luc-D3-H2LN (breast adenocarcinoma) and NCI-H460-Luc2 (large cell lung carcinoma) were purchased from Caliper. Cells were cultivated according to manufacturer's recommendations and were controlled for mycoplasma by an independent laboratory (Clean Cells). NBTXR3 (Nanobiotix) is a sterile aqueous suspension of functionalized crystal hafnium oxide (HfO<sub>2</sub>) spherical nanoparticles with a size centered on 50nm, determined by dynamic

light scattering technique (Zetasizer NanoZS, Malvern Instruments Ltd, Worcestershire, UK), bearing a marked negative surface charge (-50mV) in aqueous solution at pH 6-8,<sup>2,4</sup> estimated by zeta potential analysis (Zetasizer NanoZS). Cisplatin (CDDP) was obtained from Sigma Aldrich.

### Mice and Patient Derived Xenograft Models

Female immunodeficient NMRI-nu mice (6-weeks-old) were used for in vivo experiments (Janvier Labs), except for prostate cancer cell lines (PC-3, LNCaP, DU-145), where males have been used. For experiments with Patient Derived Xenograft LPS80T3 (obtained by direct transplantation of a poorly differentiated human grade 3 retroperitoneal malignant fibrous histiocytoma) and PAC-120 (obtained from a hormone-dependent prostate primary adenocarcinoma) models, 8-weeks-old Hsd:Athymic nude-FOXn1 female and 5-weeks-old Hsd:Athymic nude-FOXn1 male were used, respectively (XenTech). Mice were maintained under pathogen-free conditions in the animal facility. All animal experiments were carried out in compliance with French and European laws and regulations (European Directive 2010/63 EU). The local institutional animal ethics board and French Ministère de la Recherche approved all mouse experiments.

### Radiotherapy

For in vitro experiments, cells were irradiated at various doses according to the study, delivered as a single dose, using a 200kV X-ray source (NDI 226, Varian). For in vivo experiments, subcutaneous tumors were irradiated with various doses, using the same device as for in vitro experiments, excepted for PC-3 tumors irradiated using a 150kV X-ray source (CellRad, Faxitron), and NCI-H460 tumors irradiated using a 310kV X-ray source (Therapax, Agfa NDT). Selective irradiation of the tumor on mice was performed by the interposition of a lead shield, allowing full protection of the rest of the body, including proximal lymph nodes.

### Uptake Analysis by Transmission Electronic Microscopy

Cells were seeded into 6-well plates (in duplicate) at the density of 20,000 cells/cm<sup>2</sup>. Once cells were attached to the plate, different doses of NBTXR3 were added overnight, according to the cell line considered (ranging from

100 $\mu$ M to 800 $\mu$ M), as indicated on Figure 1. Cells were then pre-fixed with 2.5% glutaraldehyde in cacodylate 0.1M at pH 7.4 (Sigma Aldrich) for 2 hours. Cells were subsequently post-fixed with 1% osmium tetroxide (Sigma Aldrich) for 45 minutes, washed and dehydrated in graded concentrations of ethanol (50%, 70%, 95% and 100%) (Sigma Aldrich). Cell samples were embedded with EPON (Oxford Instruments). The resin sample block was trimmed, 90 $\mu$ m thin sectioned to thickness of 70nm, (diatome diamond knives, Euromedex). Thin sections (70nm) were collected onto 200 mesh cooper palladium grids, and counterstained with lead citrate before examination with a Zeiss EM 902 transmission electron microscope (TEM) at 80KV (UR 1196 GPL: Génomique et Physiologie de la Lactation - MIMA2 - plateau de Microscopie Electronique - Jouy-en-Josas). Microphotographs were acquired using MegaView III CCD camera and analyzed with ITEM software (Eloïse). Ten (10) cells were observed to estimate NBTXR3 nanoparticle cell uptake.

### In vitro Cell Death Analysis

For clonogenic assays, cells were seeded in triplicate into 6 well plates in a range of 200–10,000 cells/well depending on the test condition and radiation dose. Once cells were attached to the plate, 50 $\mu$ M to 800 $\mu$ M NBTXR3 was added. Different doses of X-rays were delivered 16 hours post NBTXR3 treatment. The cells were cultured up to 15  $\pm$  2 days at 37°C under 5% CO<sub>2</sub>. The colonies were fixed and stained with crystal violet (Sigma) (25% in EtOH) 2 mL/well. All colonies of 50 cells or more were then counted. For clonogenic assay with NCI-H460-Luc2 cells, the same protocol was followed except that cells were exposed to 725nM of CDDP for 6 hours or 405nM of CDDP for 16 hours. Then, the medium was replaced by fresh medium without CDDP before irradiation.

### Tumor Growth Control Experiments

For the in vivo tumor growth control assays, cells were subcutaneously injected into one flank of mice. Once the tumor had grown (50–120 mm<sup>3</sup>), mice were randomized to the different groups. A volume of NBTXR3 suspension (or vehicle) corresponding to 25% of the baseline tumor volume was injected into the tumor. After 24 hours, tumors were irradiated. The non-tumor parts of the mice were shielded by lead blocks. For chemoradiotherapy experiments with NCI-H460 cells, CDDP (1mg.kg<sup>-1</sup>) was administered by intraperitoneal injection two hours prior to RT, daily over 5 consecutive days. Length (L)

and width (W) of tumors were measured 2–3 times per week using a digital caliper. Tumor volumes were calculated using the formula (L $\times$ W<sup>2</sup>/2).

### In vivo $\mu$ CT Analysis

MicroComputerized Tomography ( $\mu$ CT) was used for visualization, evaluation of 3D dispersion and retention of NBTXR3 within the tumor. For  $\mu$ CT acquisition, mice were anesthetized using isoflurane (delivered as 1–3% for maintenance; up to 5% for induction) in oxygen from a precision vaporizer. Micro-CAT II CT scanner (Siemens) in which X-rays were generated at 80 kVp and 500 mA was used as imaging acquiring equipment (Voxcan).

### Statistical Analysis

For the clonogenic assays, the studies have been independently repeated at least three times. Results are expressed as mean of surviving fraction (SF)  $\pm$  SD. The results were analyzed by one-way ANOVA. For in vivo CDDP experimentation, tumor growth curve was analyzed using mixed linear modeling (MLM), performed with R statistics software. GraphPad Prism 7.04 software was used to perform statistical analyzes. Significance was defined at the level of  $p < 0.05$ .

## Results

### NBTXR3 is Endocytosed by Cancer Cells

The ability of tumor cell lines to internalize NBTXR3 nanoparticles was assessed by TEM in eight cell lines originating from head and neck, lung, breast and prostate cancer (Figure 1, Table 1). In all these cell lines, nanoparticles were systematically detected in the cytoplasm, where they formed clusters of various sizes distributed throughout the cell. The amount of intracellular NBTXR3 greatly varied across the cell lines analyzed. Among the prostate cancer cell lines analyzed, PC-3 internalize the most, and LNCaP internalize the least of NBTXR3 nanoparticles (Figure S1). However, no nanoparticles were observed in the nuclei, regardless of the cell line considered.

### RT-Activated NBTXR3 Kills Cancer Cells More Efficiently Than RT Alone

We sought to determine the impact of NBTXR3+RT on cell death induction, compared to RT alone. For this, we carried out clonogenicity tests on five cell lines originating from glioblastoma, prostate, liver, and pancreas cancers, varying the concentration of NBTXR3 (50–800 $\mu$ M) and the dose of

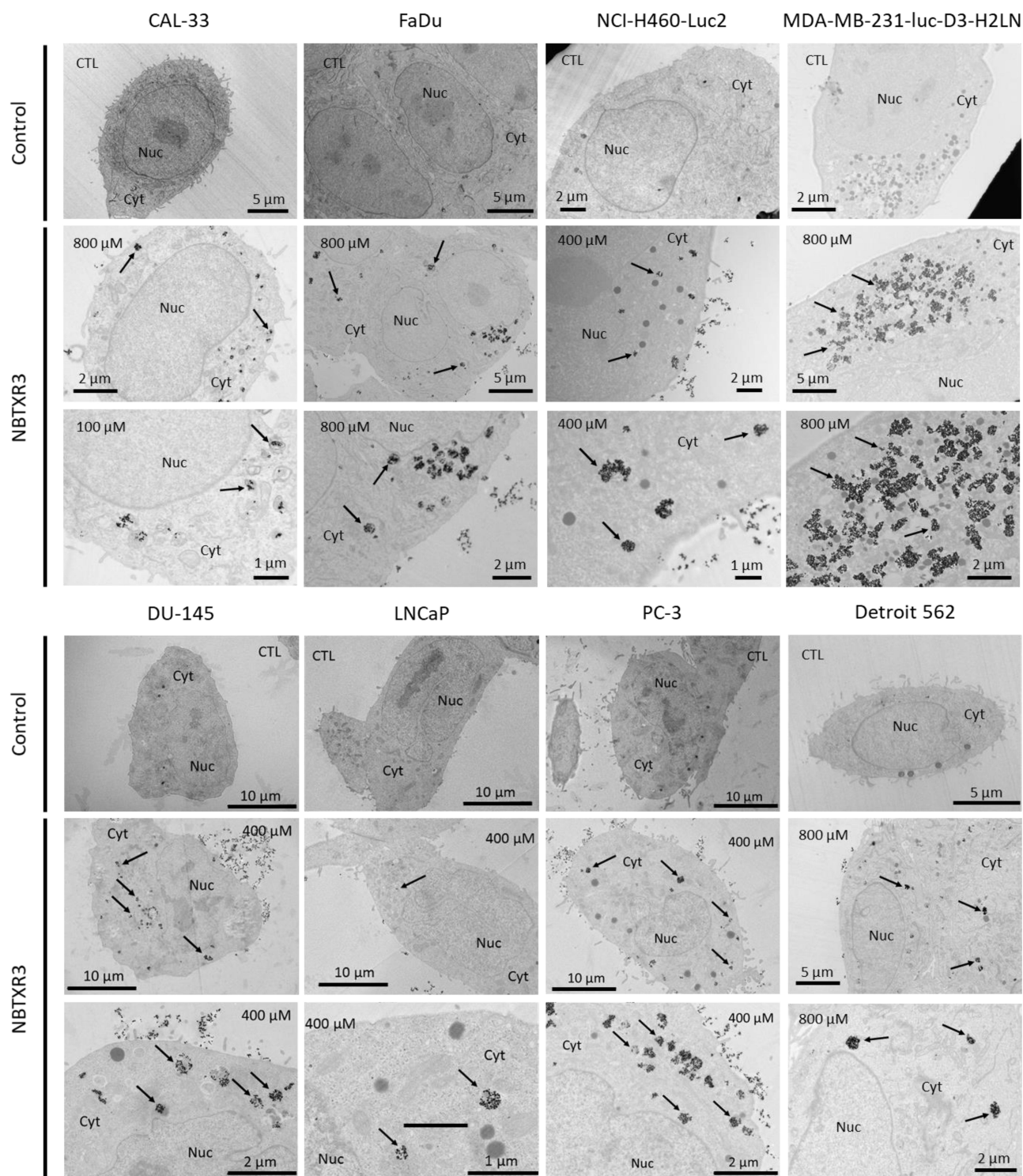


**Figure 1** NBTXR3 nanoparticles are endocytosed by cancer cells and form clusters in the cytoplasm. Transmission electronic microscopy (TEM) representative images of NBTXR3 nanoparticles uptake, forming clusters in CAL-33, FaDu, NCI-H460-Luc2, MDA-MB-231-luc-D3-H2LN (upper panel) and DU-145, LNCaP, PC-3, Detroit 562 cells (lower panel). Cells were treated overnight with NBTXR3. 100 $\mu$ M, 400 $\mu$ M and 800 $\mu$ M indicate concentrations of NBTXR3 added to cells; arrows indicate NBTXR3 clusters.

**Abbreviations:** Cyt, cytoplasm; CTL, control cells (no NBTXR3); Nuc, nucleus.

RT (1–6Gy) used (Figure 2, Table 1). No significant clonogenic toxicity of NBTXR3 without RT was observed at the tested concentrations. For all cell lines studied, a NBTXR3

dose-dependent increase in cell death was observed from 2Gy, compared to RT alone. For some concentrations of NBTXR3, this difference becomes significant, compared to

**Table 1** Compilation of Preclinical Studies Performed with NBTXR3

Tissue Origin	Cancer Type	Cell Line Name	In vitro		In vivo	
			TEM	Efficacy	$\mu$ CT	Efficacy
Brain	Glioblastoma	42MG-BA	[2, 4]	[4]		
		T98G		•		
Breast	Adenocarcinoma	MDA-MB-231-luc-D3-H2LN	•			
Colon	Carcinoma	CT26		[20]	[20]	[20]
		HCT116	[2, 4]	[4, 19]	[2, 4]	[2, 4]
	Adenocarcinoma	HT29	[4]	[4]		
Head and Neck	Tongue squamous cell carcinoma	CAL-33	•	[4]	•	•
	Pharyngeal squamous cell carcinoma	Detroit 562	•			
	Hypopharyngeal squamous cell carcinoma	FaDu	•	•, [4]	•	•
Liver	Hepatocellular carcinoma	HEP-3B		•		
Lung	Large cell lung carcinoma	NCI-H460-Luc2	•	•, [4]	•	•
Lung metastasis	Fibrosarcoma	Hs913T	[4]	[4]		
Pancreas	Carcinoma	MIA PaCa-2		•		
	Ductal adenocarcinoma	PANC-1	[4]	[4]		
Prostate	Carcinoma	DU-145	•	•	•	•
	Adenocarcinoma	LNCaP	•			
		PAC-120			•	
		PC-3	•	•	•	•
Soft tissue	Rhabdomyosarcoma	A673				[2, 4]
	Fibrosarcoma	HT1080	[2, 4]	[2, 4]		•
	Liposarcoma	LPS80T3			•	•

**Notes:** • Studies presented in this article; blank boxes indicate that the study has not been done. References of previously published data are indicated in square brackets.

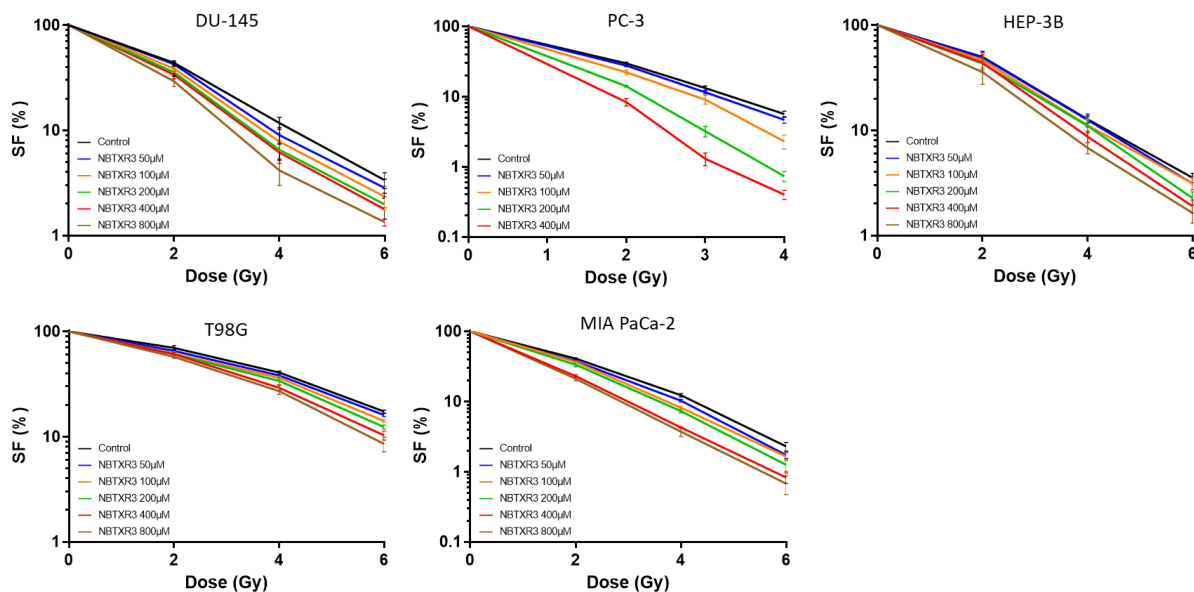
RT alone and an increase in the Dose Enhancement Factor (DEF) can be observed (Figure 2B).

## Distribution and Retention of NBTXR3 in Tumor

The intended route of administration for NBTXR3 is a single intratumoral injection.<sup>5,10</sup> For treatment with NBTXR3 to be effective, it is essential that the nanoparticles remain within the tumor throughout the RT sessions, whatever the type of solid tumor injected. Thus, we evaluated the dispersion and retention of NBTXR3 in various type of tumor at one day and several days after injection. To do this, we injected NBTXR3 into subcutaneous tumors of six different mice models (cell

lines and PDX), originating from lung, prostate, sarcoma, and head and neck cancers (Figure 3, Table 1). The high density of the nanoparticles renders them radio-opaque and easy to visualize by  $\mu$ CT (Figure 3A). NBTXR3 localization was thus assessed the day after intratumoral injection (D02) and then at different post-injection time points (Figure 3B). These studies showed that, in all tumors, nanoparticles were found well distributed inside the tumor mass the day after intratumoral injection. The  $\mu$ CT performed one or two weeks after the injection showed that the nanoparticles were still localized in the tumor. Remarkably, in the PAC-120 PDX model, which has very slow tumor growth, the nanoparticles were still present 50 days after the first  $\mu$ CT.

**A**

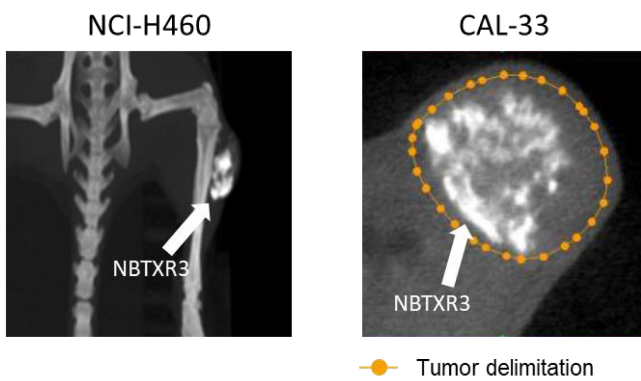


**B**

Cell line	NBTXR3 (μM)	0Gy		2Gy		4Gy		6Gy	
		SF	DEF	SF	DEF	SF	DEF	SF	DEF
DU-145	0	100	43.7±4.28			11.7±3.43		3.4±1.27	
	50	93.7±4.73	42.4±4.28	1.03±0.044		9.0±3.60	1.39±0.368	2.8±1.31	1.29±0.338
	100	89.5±8.63	38.6±6.63	1.15±0.143		7.8±3.21	1.64±0.488	2.3±1.32	1.72±0.684
	200	89.0±3.55	35.6±6.14	1.25±0.136		6.5±2.96	2.05±0.826	2.0±1.21	2.05±0.769
	400	91.7±9.35	33.6±6.26 *	1.33±0.203		6.1±2.94 *	2.22±0.912	1.8±1.23	2.37±1.028
	800	89.0±6.82	29.2±6.91 *	1.55±0.292		4.1±2.62 *	3.46±1.426	1.3±1.11	3.36±1.315
HEP-3B	0	100	49.8±14.28			12.8±2.15		3.6±0.81	
	50	108.8±15.7	49.1±12.77	1.01±0.095		12.5±3.92	1.06±0.168	3.1±0.90	1.17±0.214
	100	96.9±17.7	46.5±16.73	1.10±0.112		11.1±3.66	1.19±0.218	3.1±0.95	1.18±0.294
	200	88.9±11.6	43.1±12.34	1.17±0.112		11.0±3.51	1.21±0.219	2.3±0.74	1.68±0.624
	400	109.1±10.4	44.0±18.08	1.21±0.274		8.7±2.37	1.50±0.223	1.9±0.61 *	1.99±0.611
	800	74.9±15.7	35.6±18.56	1.63±0.606		6.8±1.81 *	1.95±0.497	1.6±0.72 **	2.46±1.113
MIA PaCa-2	0	100	40.9±1.56			12.3±1.34		2.3±0.66	
	50	95.6±3.55	37.6±2.61	1.09±0.070		10.3±0.83 *	1.20±0.052	1.7±0.36	1.34±0.180
	100	89.5±4.68	36.8±1.36	1.11±0.068		8.2±0.70 *	1.51±0.194	1.6±0.15	1.41±0.144
	200	90.3±2.23	33.4±4.84 *	1.25±0.200		7.3±0.79 *	1.69±0.121	1.2±0.45	1.91±0.250
	400	93.3±9.71	23.1±1.83 *	1.78±0.083		4.5±0.55 *	2.76±0.458	0.8±0.30 *	2.93±0.327
	800	90.1±7.72	21.1±2.72 *	1.97±0.291		3.7±1.05 *	3.58±1.449	0.7±0.39 *	4.43±2.418
PC-3	0	100	29.7±2.23			5.6±0.97		N.D.	
	50	95.3±6.3	27.6±1.68	1.08±0.061		4.7±0.86	1.23±0.324	N.D.	N.D.
	100	90.7±5.7	22.2±2.87 **	1.36±0.217		2.3±0.86 **	2.65±1.019	N.D.	N.D.
	200	89.0±7.4	14.0±0.69 **	2.13±0.263		0.7±0.23 **	8.61±4.246	N.D.	N.D.
	400	82.0±6.0	8.3 ±1.82 **	3.67±0.719		0.4±0.07 **	14.44±2.238	N.D.	N.D.
T98G	0	100	69.8 ±6.83			40.6 ±2.60		17.3±1.13	
	50	91.2±5.68	65.4±3.56	1.07±0.126		38.1±2.52	1.07±0.043	16.0±1.08	1.08±0.061
	100	86.6 ±2.75	61.7±4.85	1.14± 0.126		36.1 ± 2.31	1.12± 0.034	14.1±0.78	1.22±0.038
	200	82.9±8.75	60.7±4.08	1.15±0.121		33.9±5.53	1.22±0.147	12.3±1.06 **	1.41±0.158
	400	75.2±5.08	60.8 ±5.28	1.15± 0.146		29.1 ±3.26 **	1.40± 0.105	10.3±1.99 ***	1.72±0.290
	800	74.8±6.45	57.2±3.32 **	1.22±0.145		27±3.89 ***	1.51±0.184	8.5±2.68 ***	2.17±0.606

**Figure 2** NBTXR3 activated by RT kills more cancer cells than RT alone. **(A)** Clonogenic assay in DU-145, PC-3, HEP-3B (upper panel), T98G, and MIA PaCa-2 (lower panel). Cells were treated overnight with various concentrations of NBTXR3, then irradiated. After several days, colonies were stained using crystal violet and counted. Presented data were obtained from at least three independent experiments (n≥3). Data are represented as surviving fraction percentage (SF (%)) ± SEM. **(B)** Surviving fraction (SF) and corresponding Dose Enhancement Factor (DEF) for each condition. Percentage of surviving fraction (SF) ± SD and dose enhancement factor (DEF) ± SD. n ≥ 3. \*p<0.05; \*\*p<0.01; \*\*\*p<0.001. **Abbreviation:** N.D., not determined.

A



B

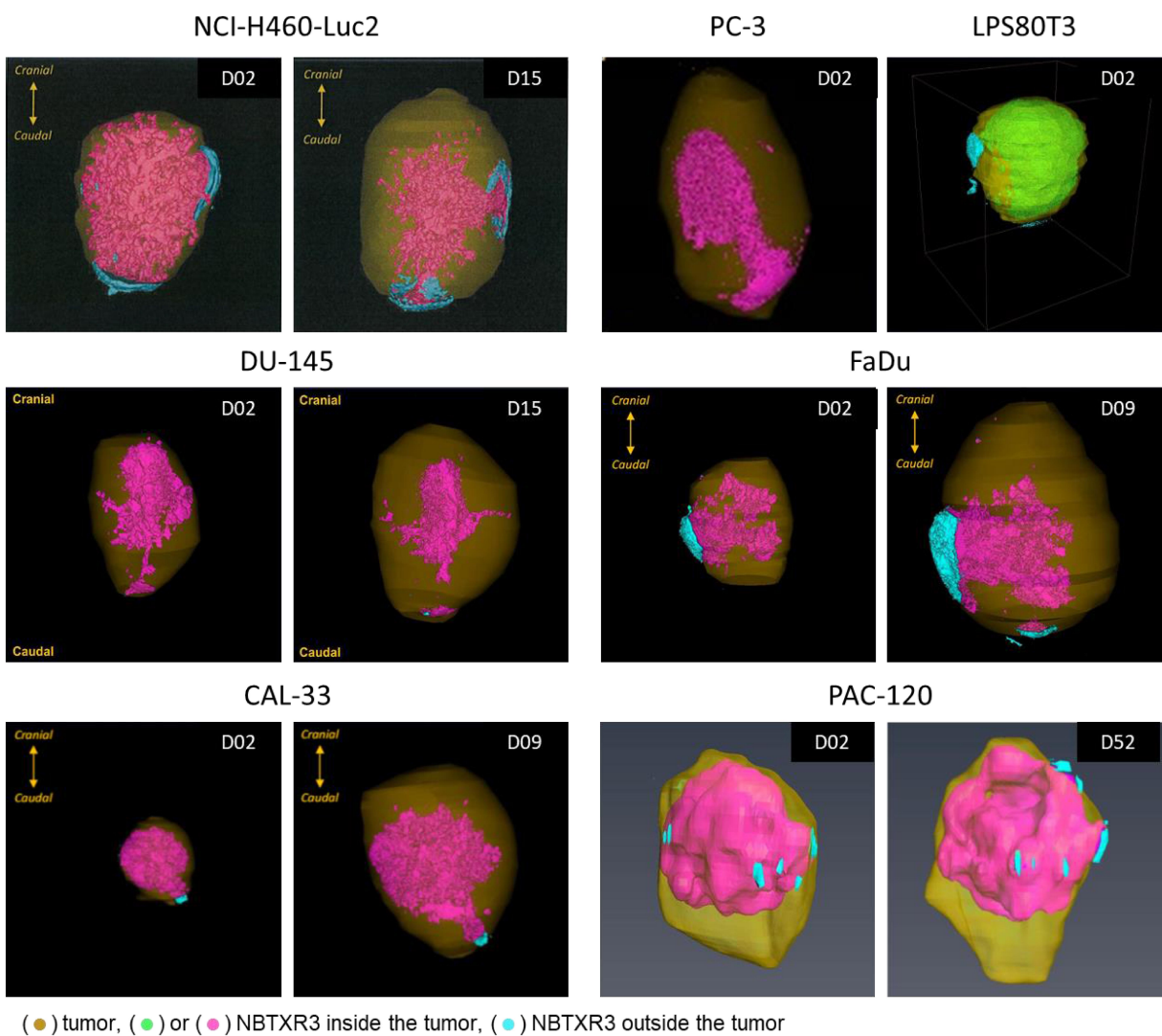


**Figure 3** After intratumoral injection, NBTXR3 distributes and remains in the tumor. **(A)** Thanks to its composition, NBTXR3 is easily observable in the tumor by  $\mu$ CT (white areas indicated by the arrows). **(B)** 3D representation of the of NBTXR3 nanoparticles distribution within tumor tissues of models NCI-H460-Luc2, PC-3 and LPS80T3 (upper panel), DU-145, FaDu (middle panel), CAL-33 and PAC-120 (lower panel), after  $\mu$ CT analysis. Indicated day corresponds to time post-intratumoral injection (D01).

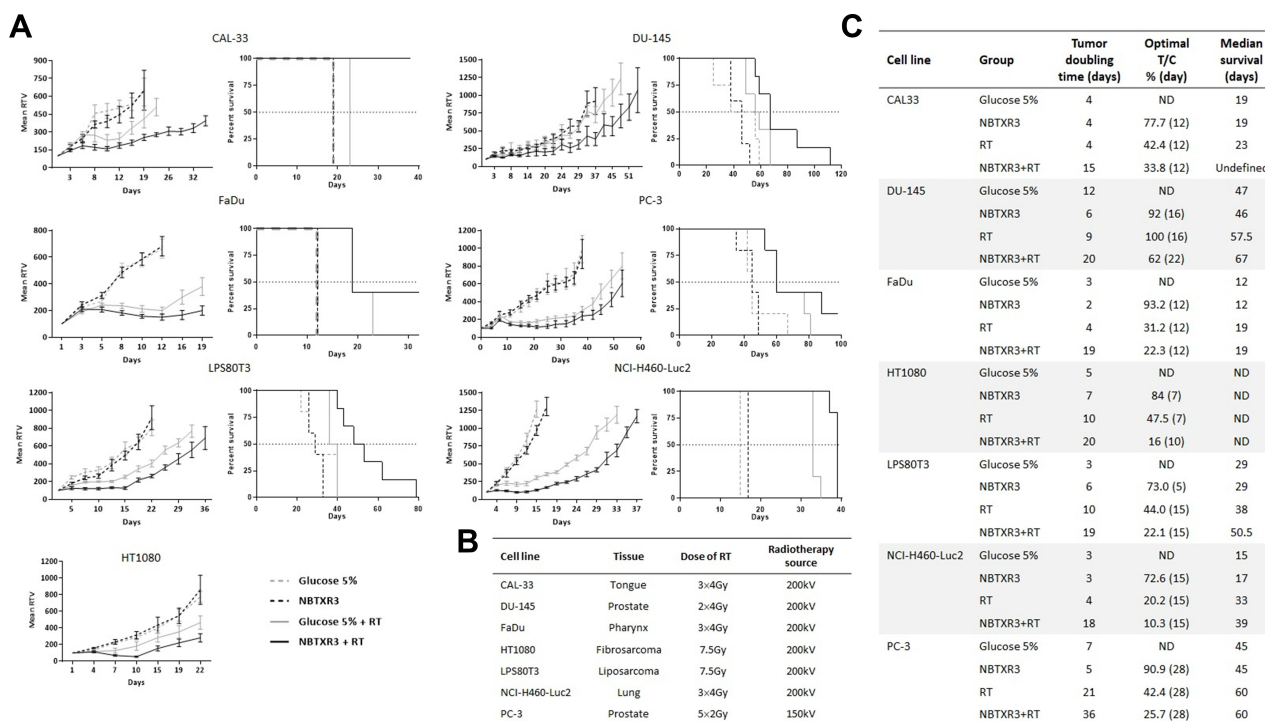


**Figure 4** NBTXR3 activated by radiotherapy controls tumor growth more effectively than radiotherapy alone. **(A)** The ability of NBTXR3 to control tumor growth better than radiotherapy as well as the impact on survival was tested in nude mice bearing a tumor of CAL-33, FaDu, LPS80T3, HT1080 (left column), DU-145, PC-3 and NCI-H460-Luc2 (right column). Number of mice per group: 5–6. Tumor growth curves are expressed as mean relative tumor volume (RTV) ± SEM. **(B)** Table indicative of the types of cancers tested, the doses of RT used and the source of radiotherapy. **(C)** Tumor doubling time, optimal T/C and median survival of the in vivo experiment results.

## RT-Activated NBTXR3 Improves Tumor Growth Control

To confirm the ability of NBTXR3 to destroy tumor cells more efficiently than RT alone in vivo, we used seven human cell lines, derived from six distinct tumor types (tongue, prostate, pharynx, fibrosarcoma, liposarcoma and lung), subcutaneously injected in nude mice (Figure 4, Table 1). In the absence of RT, the injection of NBTXR3 did not affect tumor growth, thus confirming the inert nature of these nanoparticles in their “off” status observed in vitro (Figure 4A and C). In contrast, treatment with NBTXR3+RT better controlled tumor growth and improved survival regardless of the model considered, compared to radiotherapy alone (Figure 4). NBTXR3+RT thus markedly increased the doubling time of tumor growth, the median survival, and reduced the optimal T/C (Figure 4C). Only the FaDu and PC-3 models did not show an improvement in their median survival, but an increase in overall survival could still be observed (Figure 4A and C). In the well-known radioresistant DU-145 tumor model,<sup>11–13</sup> RT (2×4Gy) had no significant effect on tumor growth. In stark contrast, the treatment

of DU-145 tumors by RT-activated NBTXR3 resulted in a strong tumor growth delay. The tumor doubling time increased from 9 to 20 days, for RT and NBTXR3+RT, respectively (Figure 4A and C).

## NBTXR3 Improves the Efficacy of Chemoradiotherapy with Cisplatin

We sought to determine the ability of NBTXR3 to improve the effectiveness of chemoradiation with cisplatin (CDDP+RT). We first performed clonogenicity tests using the NCI-H460-Luc2 cell line. Cells were treated with the CDDP 6h or 16h before RT, in the presence or not of NBTXR3, to highlight a possible time effect. The results show that NBTXR3+RT was as effective as CDDP+RT at destroying cancer cells (Figure 5A and B). Interestingly, the addition of NBTXR3 to CDDP+RT treatment significantly improved cell destruction, whatever the time considered. We then compared the effects of RT, CDDP+RT, NBTXR3+RT and NBTXR3+CDDP+RT treatments on tumor growth control, in mice bearing an NCI-H460 tumor (Figure 5C). The tumor growth delay was extended for mice receiving NBTXR3 activated by radiotherapy or



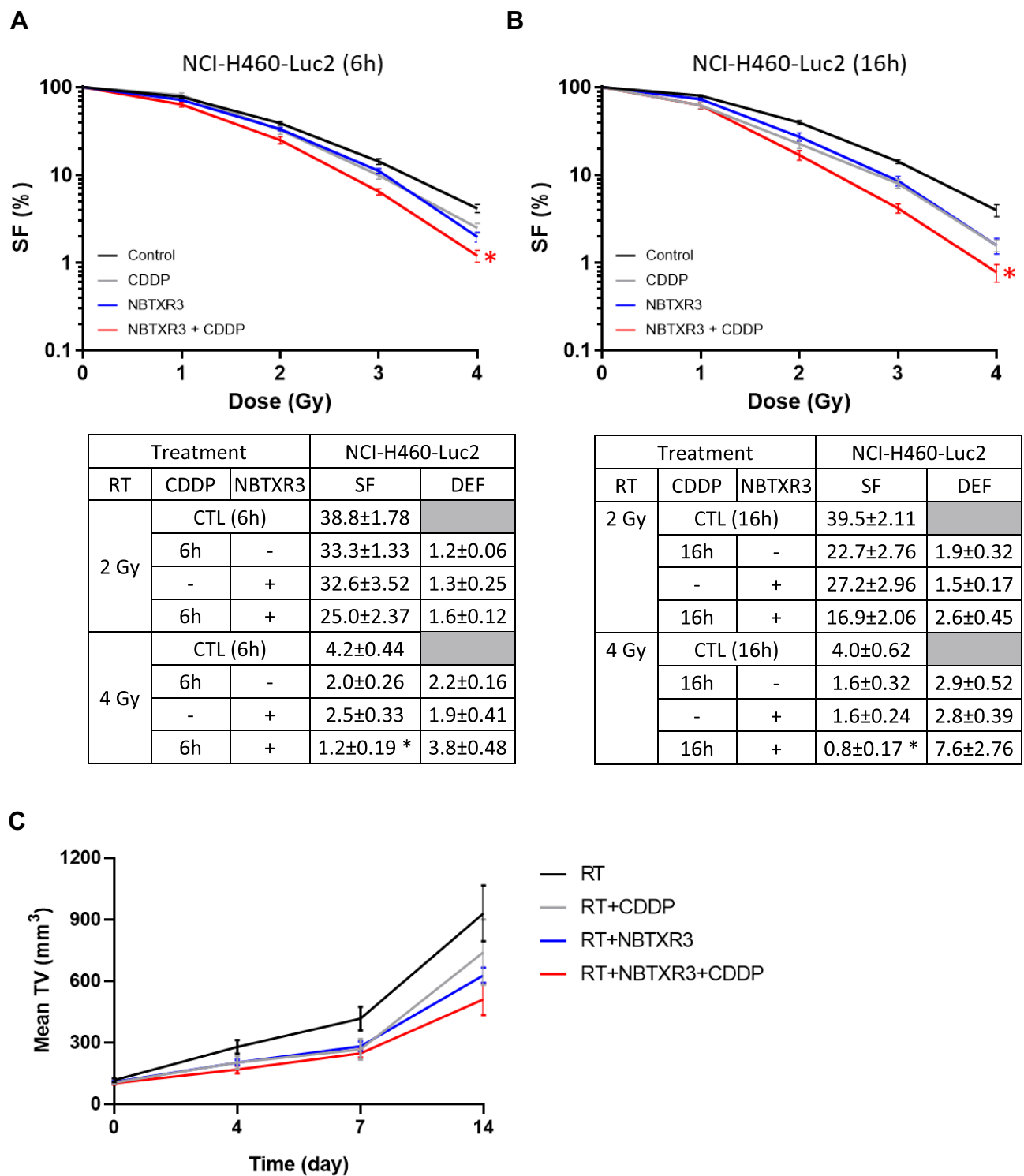


**Figure 5** RT-activated NBTXR3 improves the efficacy of cisplatin. The capacity of NBTXR3 to kill cancer cells, in combination or not with cisplatin (725nM of CDDP for 6 hours or 405nM of CDDP for 16 hours), was analyzed by clonogenic assay on the NCI-H460-Luc2 cell line, after an incubation of 6h (A) or 16h (B) with cisplatin before irradiation. Presented data were obtained from five independent experiments (n=5). Data are represented as surviving fraction percentage (SF (%)) ± SEM. Surviving fraction (SF) and corresponding Dose Enhancement Factor (DEF) for each condition are indicated and time point are indicated on the lower panel. \* $p < 0.05$  vs CTL. (C) The ability of NBTXR3 to control tumor growth was compared in combination or not with cisplatin (CDDP, 1mg.kg<sup>-1</sup>). Tumor growth curves are expressed as mean tumor volume (TV) ± SEM. Number of mice per group: 5.

cisplatin and radiation, compared with mice receiving radiation alone (~17 days versus ~22 days). Histology analyses revealed that NBTXR3+RT reduced cell proliferation and induced apoptosis, similarly to CDDP+RT ([Supplementary Materials](#) and [Methods](#) and [Figure S2](#)). NBTXR3 +CDDP+RT treatment markedly prolonged tumor growth compared with RT alone (~17 days versus ~25 days delay).

## Discussion

The first-in-class nanosized radioenhancer NBTXR3 has been developed to multiply the effects of RT without generating additional side effects.<sup>5,10,14</sup> Its effectiveness has been recently successfully demonstrated in a Phase II/III clinical study in locally advanced soft tissue sarcomas.<sup>5</sup> In the preclinical studies presented in this article, we wanted to demonstrate that NBTXR3 can be used to treat any type of solid cancer, and that its combination with chemoradiotherapy treatments can improve their effectiveness.

A cellular uptake of NBTXR3 was evidenced by TEM in all height cancer cell lines studied originating from different organs (pharynx, tongue, lung, breast, and prostate). The number of nanoparticles detected in the cytoplasm varies depending on the cell line used, similar to previously published data.<sup>4</sup> These differences cannot be explained by the organ origin of the cells, since such a difference can be observed between the PC-3 and LNCaP cell lines, both originating from prostate cancer ([Figure S1](#)). We hypothesize that this could be due to various internalization capacities between cell lines, eg, the clathrin-mediated endocytosis pathway, known to be an important entry point for internalization of nanoparticles,<sup>15</sup> but additional analyses must be performed to confirm this. Another shared characteristic observed in TEM analysis was the capacity of all cell lines to form nanoparticle clusters in their cytoplasm. This concentration of the nanoparticles suggests a common intracellular trafficking mechanism. Autophagy may possibly explain nanoparticle aggregates because this process is frequently activated by nanoparticles.<sup>16</sup> However, this may not be the only process involved since nanoparticle aggregates were also observed in the autophagy-deficient DU-145 cell line ([Figure 1](#)).<sup>17</sup> Additional experiments are required to identify the endocytosis and intracellular trafficking pathways involved. In addition, nanoparticles have never been observed in the nucleus of cells, which could be explained by their size (centered on 50 nm). Indeed, it has previously

been reported by Wu et al<sup>18</sup> that only <50nm silver nanoparticles can enter the nucleus. Considering previously published results,<sup>2,4</sup> the analyzes carried out in fourteen cell lines from ten different organs/tissues clearly show that the endocytosis of NBTXR3 nanoparticles, as well as their clustering and exclusion from the nucleus are characteristics universally shared between cancer cell lines ([Table 1](#)).

All the clonogenic assays presented in this article show that NBTXR3+RT increased cancer cell death, in a dose-dependent manner, compared to the same dose of RT alone. Considering previous studies,<sup>2,4,19,20</sup> the enhancement of cell death following NBTXR3+RT treatment compared to RT alone has now been demonstrated in fifteen different cancer cell lines originating from nine different organs/tissues ([Figure 6](#), [Table 1](#)). This also clearly demonstrates that, thanks to its radioenhancing capacity, NBTXR3 can kill any type of cancer cell. It is assumed that this is also the case for any other solid tumor cancer cells. This superior capacity of NBTXR3 activated by RT to destroy cancer cells, compared to RT alone, could make it possible to reduce the dose per fraction, while maintaining the same efficacy. This could have direct applications for patients, helping to limit the side effects of RT, thereby improving the patient's quality of life and costs to the healthcare system. The improvement in cell death goes beyond a simple decrease in the number of cancer cells. Indeed, the heightened release of tumor-associated antigens triggered by NBTXR3+RT treatment could play a critical role in the priming or amplification of the adaptive antitumor immune response, as recently reported in the CT26 mouse colorectal model.<sup>20</sup>

Preclinical and clinical studies have not revealed any leakage of NBTXR3 into surrounding tissues and showed that NBTXR3 remains within the tumor throughout RT treatment.<sup>2,10,20</sup> To expand these results, we examined the retention of NBTXR3 in seven different tumor models by  $\mu$ CT. We demonstrate that NBTXR3 was detectable within the tumor from few days to several weeks after intratumoral injection. Considering previously published preclinical data, the retention of NBTXR3 nanoparticles in tumor has been demonstrated in nine different cancer cell lines originating from six different organs/tissues ([Figure 6](#), [Table 1](#)). We postulate that the "long-term" retention of NBTXR3 observed in these tumors could be due, at least in part, to the internalization of the nanoparticles by cells, as demonstrated in the different TEM analysis, but additional studies are needed to confirm this hypothesis.

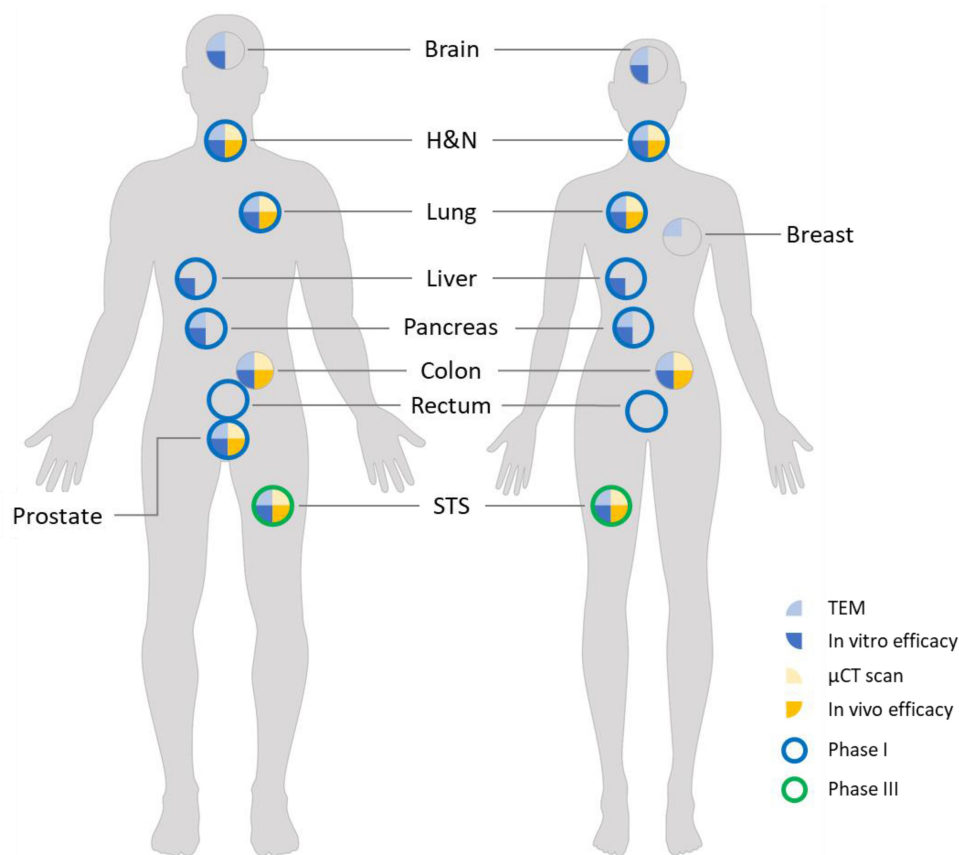


**Figure 6** Review of studies with NBTXR3. The various experiments carried out in vitro and in vivo on the various human models demonstrated the effectiveness of NBTXR3 and its capacity to treat any kind of solid tumor. These preclinical results have been confirmed in a Phase II/III clinical trial in patients with soft tissue sarcoma, and other Phase I trials are currently in progress.

Nonetheless, we can conclude that the distribution and retention of NBTXR3 in solid tumors are universal phenomena.

NBTXR3 nanoparticles have been designed to act as radioenhancers, only producing an antitumor effect when they receive ionizing radiation (“on” status). Without RT (“off” status), the nanoparticles are then “inert”. The difference between “off” and “on” status were previously reported<sup>2,4,19</sup> and confirmed here by in vitro clonogenicity studies. These properties have also been demonstrated in vivo<sup>2,20</sup> and confirmed by the new studies presented here. The “off” status of NBTXR3 had no effect on tumor growth, compared to the control, whatever the model considered. In contrary, the tumor growth control was systematically improved in the presence of NBTXR3+RT (“on” status), compared to RT alone, even in a radioresistant tumor model. These results are in good agreement with the previously published results<sup>2,5,20</sup> and support the possibility that, thanks to its physical mode of

action, the antitumor efficacy of NBTXR3 could be efficient in any type of solid tumor.

Carcinoma of the lung is the leading cause of cancer-related death in both men and women,<sup>21</sup> non-small cell lung cancer (NSCLC) accounting for almost 75% of cases.<sup>22</sup> Concurrent chemoradiotherapy using cisplatin (CDDP) regimen is currently the standard treatment for stage III inoperable NSCLC.<sup>23,24</sup> For elderly patients inoperable and too frail to support treatment with cisplatin, RT is the only therapeutic alternative, whose beneficial effects are limited. Based on its very good safety profile reported in patients,<sup>10</sup> NBTXR3 could open new avenues for the treatment of these particularly frail patients. In fact, the clonogenicity assays with CDDP or NBTXR3, in combination with RT, show that NBTXR3+RT is as efficient as CDDP+RT treatment to kill cancer cells. On the other hand, similar efficacies were obtained for both treatments in vivo. These promising results are now tested in a Phase I clinical trial to treat patients too frail to receive chemoradiotherapy with CDDP, and

eligible only for RT (NCT02901483). Remarkably, in vitro and in vivo results of CDDP+NBTXR3+RT show that this combination improved the efficacy of CDDP+RT. This suggests that patients usually treated with this chemoradiotherapy could benefit from the addition of NBTXR3 in their treatment. These results also open up interesting new perspectives concerning the combination of NBTXR3 with other chemoradiotherapies, such as, g, poly(ADP-ribose)polymerase inhibitors (PARPi)<sup>25</sup> or tyrosine kinase inhibitors (TKI).<sup>26</sup> NBTXR3 activated by RT may also be valuable in combinations with other therapies, such as immune checkpoint inhibitors like anti-PD-1. Indeed, we recently showed in immunocompetent mice that NBTXR3 activated by RT was able to induce an antitumor immune response, producing an abscopal effect.<sup>20</sup>

Taken together, the data presented so far support the possibility that NBTXR3 could be universally used with RT to treat any type of solid cancer.<sup>2,4,5,10,19,20</sup> NBTXR3 opens promising new therapeutic perspectives of treatment for the benefit of millions of patients. Several clinical trials in HNSCC, liver cancers, as a single agent, or in combination with chemotherapy in HNSCC and rectal cancer as well as in combination with anti-PD-1 in HNSCC, lung or liver metastasis from any primary cancer are currently in progress to confirm the important therapeutic potential of NBTXR3.

## Abbreviations

CDDP, cisplatin; DEF, dose enhancement factor; HNSCC, head and neck squamous-cell carcinoma; PARPi, poly(ADP-ribose) polymerase inhibitor; RT, radiotherapy; SF, surviving fraction; TEM, transmission electron microscopy; TKI, tyrosine kinase inhibitor;  $\mu$ CT, X-ray micro-computed tomography.

## Acknowledgments

The authors thank Dr Joëlle Morvan, Senior Manager, Scientific Advisor and Medical Writer and Dr Omar Vivar, Senior Manager, Medical Writer at Nanobiotix for proofreading this article and wise advice.

## Disclosure

P. Zhang, J. Marill, A. Darmon, N. Mohamed Anesary, and S. Paris are full employees of Nanobiotix. The authors report no other conflicts of interest in this work.

## References

- Barton MB, Frommer M, Shafiq J. Role of radiotherapy in cancer control in low-income and middle-income countries. *Lancet Oncol.* 2006;7(7):584–595. doi:10.1016/S1470-2045(06)70759-8
- Maggiorella L, Barouch G, Devaux C, et al. Nanoscale radiotherapy with hafnium oxide nanoparticles. *Future Oncol.* 2012;8(9):1167–1181. doi:10.2217/fon.12.96
- Pottier A, Borghi E, Levy L. New use of metals as nanosized radioenhancers. *Anticancer Res.* 2014;34(1):443–453.
- Marill J, Anesary NM, Zhang P, et al. Hafnium oxide nanoparticles: toward an in vitro predictive biological effect? *Radiat Oncol.* 2014;9:150. doi:10.1186/1748-717X-9-150
- Bonvalot S, Rutkowski PL, Thariat J, et al. NBTXR3, a first-in-class radioenhancer hafnium oxide nanoparticle, plus radiotherapy versus radiotherapy alone in patients with locally advanced soft-tissue sarcoma (Act.In.Sarc): a multicentre, Phase 2-3, randomised, controlled trial. *Lancet Oncol.* 2019;20(8):1148–1159. doi:10.1016/S1470-2045(19)30326-2
- Chithrani DB, Jelveh S, Jalali F, et al. Gold nanoparticles as radiation sensitizers in cancer therapy. *Radiat Res.* 2010;173(6):719–728. doi:10.1667/RR1984.1
- Chow JC, Leung MK, Jaffray DA. Monte Carlo simulation on a gold nanoparticle irradiated by electron beams. *Phys Med Biol.* 2012;57(11):3323–3331. doi:10.1088/0031-9155/57/11/3323
- Cui L, Her S, Borst GR, Bristow RG, Jaffray DA, Allen C. Radiosensitization by gold nanoparticles: will they ever make it to the clinic? *Radiother Oncol.* 2017;124(3):344–356. doi:10.1016/j.radonc.2017.07.007
- Scher N, Bonvalot S, Le Tourneau C, et al. Review of clinical applications of radiation-enhancing nanoparticles. *Biotechnol Rep.* 2020;28:e00548. doi:10.1016/j.btre.2020.e00548
- Bonvalot S, Le Pechoux C, De Baere T, et al. First-in-human study testing a new radioenhancer using nanoparticles (NBTXR3) activated by radiation therapy in patients with locally advanced soft tissue sarcomas. *Clin Cancer Res.* 2017;23(4):908–917. doi:10.1158/1078-0432.CCR-16-1297
- Leith JT, Quaranto L, Padfield G, Michelson S, Herbergs A. Radiobiological studies of PC-3 and DU-145 human prostate cancer cells: x-ray sensitivity in vitro and hypoxic fractions of xenografted tumors in vivo. *Int J Radiat Oncol Biol Phys.* 1993;25(2):283–287. doi:10.1016/0360-3016(93)90350-5
- Seifert M, Peitzsch C, Gorodetska I, Borner C, Klink B, Dubrovskaya A. Network-based analysis of prostate cancer cell lines reveals novel marker gene candidates associated with radioresistance and patient relapse. *PLoS Comput Biol.* 2019;15(11):e1007460. doi:10.1371/journal.pcbi.1007460
- Jayakumar S, Kunwar A, Sandur SK, Pandey BN, Chaubey RC. Differential response of DU145 and PC3 prostate cancer cells to ionizing radiation: role of reactive oxygen species, GSH and Nrf2 in radiosensitivity. *Biochim Biophys Acta.* 2014;1840(1):485–494. doi:10.1016/j.bbagen.2013.10.006
- Hoffmann C, Calugaru V, Borcoman E, et al. Phase I dose-escalation study of NBTXR3 activated by intensity-modulated radiation therapy in elderly patients with locally advanced squamous cell carcinoma of the oral cavity or oropharynx. *Eur J Cancer.* 2021;146:135–144. doi:10.1016/j.ejca.2021.01.007
- Foroozandeh P, Aziz AA. Insight into cellular uptake and intracellular trafficking of nanoparticles. *Nanoscale Res Lett.* 2018;13(1):339. doi:10.1186/s11671-018-2728-6
- Guo L, He N, Zhao Y, Liu T, Deng Y. Autophagy modulated by inorganic nanomaterials. *Theranostics.* 2020;10(7):3206–3222. doi:10.7150/thno.40414

17. Ouyang DY, Xu LH, He XH, et al. Autophagy is differentially induced in prostate cancer LNCaP, DU145 and PC-3 cells via distinct splicing profiles of ATG5. *Autophagy*. 2013;9(1):20–32. doi:10.4161/auto.22397
18. Wu M, Guo H, Liu L, Liu Y, Xie L. Size-dependent cellular uptake and localization profiles of silver nanoparticles. *Int J Nanomed*. 2019;14:4247–4259. doi:10.2147/IJN.S201107
19. Marill J, Mohamed Anesary N, Paris S. DNA damage enhancement by radiotherapy-activated hafnium oxide nanoparticles improves cGAS-STING pathway activation in human colorectal cancer cells. *Radiother Oncol*. 2019;141:262–266. doi:10.1016/j.radonc.2019.07.029
20. Zhang P, Darmon A, Marill J, Mohamed Anesary N, Paris S. Radiotherapy-activated hafnium oxide nanoparticles produce abscopal effect in a mouse colorectal cancer model. *Int J Nanomed*. 2020;15:3843–3850. doi:10.2147/IJN.S250490
21. Bade BC, Dela CCS. Lung Cancer 2020: epidemiology, etiology, and prevention. *Clin Chest Med*. 2020;41(1):1–24. doi:10.1016/j.ccm.2019.10.001
22. Molina JR, Yang P, Cassivi SD, Schild SE, Adjei AA. Non-small cell lung cancer: epidemiology, risk factors, treatment, and survivorship. *Mayo Clin Proc*. 2008;83(5):584–594. doi:10.1016/S0025-6196(11)60735-0
23. Eberhardt WE. Concurrent chemoradiotherapy in stage III non-small-cell lung cancer: what is the best regimen? *J Clin Oncol*. 2015;33(6):532–533. doi:10.1200/JCO.2014.58.9812
24. Tabchi S, Blais N, Campeau MP, Tehfe M. Single-center comparison of multiple chemotherapy regimens for concurrent chemoradiotherapy in unresectable stage III non-small-cell lung cancer. *Cancer Chemother Pharmacol*. 2017;79(2):381–387. doi:10.1007/s00280-016-3226-0
25. Jannetti SA, Zeglis BM, Zalutsky MR, Reiner T. Poly(ADP-Ribose) polymerase (PARP) inhibitors and radiation therapy. *Front Pharmacol*. 2020;11:170. doi:10.3389/fphar.2020.00170
26. Borghetti P, Bonu ML, Roca E, et al. Radiotherapy and tyrosine kinase inhibitors in stage IV non-small cell lung cancer: real-life experience. *Vivo*. 2018;32(1):159–164.

## International Journal of Nanomedicine

Dovepress

### Publish your work in this journal

The International Journal of Nanomedicine is an international, peer-reviewed journal focusing on the application of nanotechnology in diagnostics, therapeutics, and drug delivery systems throughout the biomedical field. This journal is indexed on PubMed Central, MedLine, CAS, SciSearch®, Current Contents®/Clinical Medicine,

Journal Citation Reports/Science Edition, EMBase, Scopus and the Elsevier Bibliographic databases. The manuscript management system is completely online and includes a very quick and fair peer-review system, which is all easy to use. Visit <http://www.dovepress.com/testimonials.php> to read real quotes from published authors.

Submit your manuscript here: <https://www.dovepress.com/international-journal-of-nanomedicine-journal>